Fully Automated Self-calibrating Hybrid Flow Analyzer for Gaseous Formaldehyde

In-Yong Eom, Qingyang Li, Jianzhong Li

Department of Chemistry and Biochemistry, Texas Tech University, Lubbock, TX 79400-1061, USA

Purnendu K. Dasgupta*

Department of Chemistry, The University of Texas at Arlington

Arlington, TX 76019-0065

Abstract

We report fully automated self-calibrating formaldehyde analyzers relying on a hybrid flow format and include operational scheme and design details. Long-term operation is made possible with the use of syringe pumps. Four identical analyzers were built and showed low LODs of 120 pptv or better (S/N =3) and good linearity over 0-50 ppbv HCHO concentration range ($r^2 \geq 0.9960$). The analyzer can resume normal operation after short-term power failure with at most two cycles of data loss following restart. Good agreement between analyzers was observed for either indoor or outdoor measurements.

The use of an integrated HCHO calibration source and full control by the host computer via a graphical user interface program enables the instrument to switch between zero, calibration and sampling modes in a programmed automated manner. Detailed field data from deployment in three urban Texas locations from the summer of 2006 are presented and some features of the data are briefly discussed.

1. Introduction

Formaldehyde (HCHO) is ubiquitous in both indoor and outdoor air. It is a known animal carcinogen; the US Environmental Protection Agency (EPA) has also designated it as a suspected human carcinogen (US Environmental Protection Agency, 2006). It is one of the most important indoor pollutants because of its extensive use in adhesives, bonding and laminating agents, urea-formaldehyde foam insulation, fabrics, coatings, plywood, and paints. It is also produced by fuel-burning appliances and from cigarettes. Elevated levels of HCHO, up to 300 parts per billion by volume (ppbv), have been reported in indoor air (US Environmental Protection Agency, 2007). Exposure to HCHO can cause watery eyes, burning sensations in eyes and throat, nausea, fatigue, difficulty in breathing, and skin rash.

Of greater importance to us is that formaldehyde is the most abundant gaseous carbonyl compound in ambient air. Aside from production from photooxidation of isoprene (Ohira et al., 2007) emitted by green vegetation, formaldehyde is a key indicator of atmospheric photochemical processes. Oxidation of volatile organic compounds in general by •OH and ozonolysis of terminal olefins in particular are well known pathways to HCHO production (Wert et al., 2003a). Incomplete fossil fuel combustion and primary industrial emissions are also considered significant sources for HCHO. Air quality has improved across the US by and large since the 80's. However, atmospheric HCHO levels measured in a industrial emission impacted area in Houston TX in 2000 exceeded 47 ppbv (Dasgupta et al., 2005), twice the highest levels measured in urban Los Angeles in the late 80's (Lawson, et. al., 1990). The interest in routine unattended measurement of HCHO therefore remains current.

1.1. Analytical Approaches

Many analytical methods have been developed for the measurement of gaseous HCHO. The topic has been reviewed by us twice in this decade (Li et al., 2001, Li et al., 2005). Briefly, direct spectroscopic techniques are the reference methods of choice. Diode laser absorption spectroscopy can be used to measure many atmospheric trace gases, including HCHO, with high specificity as the source can be tuned with very high resolution over several tens of wave numbers (Roller et al., 2006, Wert et al., 2003b). Differential optical absorption spectroscopy (DOAS) is also popular for atmospheric gas analysis because it can analyze various gases at the same time (Lee et al., 2005, Grutter et al., 2005, Wert et al., 2003a). Derivatization followed by chromatographic analysis is also commonly used to measure gaseous HCHO (US Environmental Protection Agency, 1999; Koziel et al., 2001; Wang et al., 2005). Inexpensive hanging drop instrumentation based on colorimetric and fluorometric chemistries capable of measuring ambient HCHO have been put forward (Pereira and Dasgupta, 1997; Pretto et al., 2002).

In this laboratory, we have spent more than two decades after the measurement of HCHO as well as calibration of such instrumentation (Dong and Dasgupta, 1986a,b, 1987; Dasgupta, 1987; Dasgupta et al., 1988; Zhang and Dasgupta, 1991; Fan and Dasgupta, 1994; Li et al., 2001; Li et al., 2005) The measurement approach has centered on fluorescence derivatization involving the Hantzsch reaction, which involves the cyclization of a -diketones with formaldehyde and ammonia in a slightly acidic solution at elevated temperature to form a dihydropyridine derivative. Among other -diketones, acetylacetone (2,4-pentanedione (PD)) has emerged as the reagent of choice: it reacts at a lower temperature than the others and is not affected by H_2O_2, even when the latter is present at high relative concentrations (Li et al., 2005). The chemistry and the approach display sufficient specificity for gaseous and aqueous formaldehyde measurement, as evidenced from numerous field intercomparisons (Kleindienst et al., 1988. Lawson et al., 1990; Dasgupta et al., 1990; Gilpin et al., 1997; Dasgupta et al., 2005)

1.2. Needs for improvement

The extant approach to Nafion® diffusion scrubber collected, PD-chemistry based solid state light emitting diode (LED) excited fluorometric measurement of HCHO, where the input alternates between sample and zero every few minutes to produce a pulsed output of HCHO response provides a very affordable, simple but sensitive alternative to direct spectroscopic measurements; a commercial version is also available (www.alphaomegapt.com/methanalyzer.htm). However, it would be highly desirable to improve on several independent issues related to this approach. The first of these concerns the issue of multichannel peristaltic pumps; the flow rates produced by such compressible tubing based pumps gradually change and the tubing must be replaced every 1-2 weeks. There are no provisions for automated periodic calibration. In addition, as is true for any liquid reagent based analyzer, it will be highly desirable to minimize liquid consumption, especially when high time resolution is not needed. Finally, power failure in field locations are common; even when power returns, most wet instrumentation do not properly recover to start producing reliable data again.

We propose here a new instrument that fully meets these desired criteria. In part, we borrow from the recent hybrid flow analyzer concept introduced for ammonia measurement (Amornthammarong et al., 2006). The flow configuration is a hybrid flow between continuous flow as used in our previous HCHO analyzers and sequential injection flow modes (see e.g., Liu and Dasgupta, 1995) that readily permit the use of syringe pumps (Samanta et al., 2003). Multiple identical analyzers are built and tested in a collocated manner. Finally we deploy these instruments in three urban areas in Texas for a sustained period of time and present the resulting data.

2. Experimental section

2.1. System description

The analyzer consists of four modules: HCHO-free air supply (zero air), calibration source, formaldehyde measurement instrument itself, and the data acquisition and control system. The arrangement and the liquid and gas flow are schematically shown in Figure 1. The whole system is contained in a minitower size computer case with the exception of the zero air supply, the diffusion scrubber (DS), and a laptop personal computer (PC).

2.2. Primary analyzer

The HCHO-free gas source (zero air, not shown in Figure 1) is used continuously to provide low maintenance flow to the HCHO calibration chamber CC and at much greater flow rates during calibration. The calibrant chamber CC is machined from aluminum block AL (1 x 3 x 5 inch) shown in Figure 2; AL consists of two chambers. The smaller gastight chamber is the calibrant chamber CC; it holds the permeation tube source PT (www.vicimetronics.com). The chamber top has a polyvinyledene fluoride (PVDF) screw cap SC sealed to CC by O-ring OR and equipped with a flat-seat ¼-28 threaded aperture. Capillary restrictor CR2 (1.6 mm o.d., 0.10 mm i.d., 30 mm long, PEEK), affixed with a compression nut and ferrule MN provides the gas exit from CC and terminates in the common port of SV1 (648K031, www.nresearch.com). The larger main chamber in AL is a hollowed out 3 x 3.2 in. rectangular area which holds a sandwich: Two flexible, serially connected 3x3 in. siliconized heaters SH (www.watlow.com) providing 22.5 W@110V forms the outer layer. A temperature controller (CN8592-R1-T2, Omega Engineering) is used to set and monitor the thermostated enclosure via the platinum RTD sensor embedded in the wall of CC. The CC was maintained at 60 °C in this work. There are two inner layers between the two heaters: The first is 60 cm length of shaped 3/8" copper tubing CT serving as a thermal equilibration conduit. Zero air continuously flows via entrance capillary CR1 (1.6 mm o.d., 0.10 mm i.d., 90 mm long, PEEK), metal union MU, into CT at ~20 ml/min and enters CC through an O-ring seal. The second inner layer consists of a heated reactor (HR) composed of 4.5 m of 30 ga. (30 SW, 0.3 mm id, www.zeusinc.com) PTFE tubing in a serpentine –II pattern (Waiz et al., 2005) knitted on a 3 x 3 inch stainless steel wire mesh (1 mm grid) potted in turn in a low-melting bismuth-tin alloy (Cerrobase 5550-1, Canfield Technologies, Sayreville, NJ) in a rectangular form (3 by 3 inch, 5 mm thickness). The reactor has an internal volume of ~330 μl and under the presently stated flow rates has a residence time of 106 s. The whole assembly is put with insulating foam inside a 3 x 5 x 7 in. plastic enclosure.

Referring to Figure 1, the permeation chamber output is vented through solenoid valve SV1 to the

outside. When venting outside is impractical, (it can be vented through a room temperature oxidative catalyst, e.g., Carulite 110TR (www.caruscorporation.com). During the calibration period, SV1 is turned on so the HCHO source output is delivered to mixing tee MT1 and 1 - 10 standard liters per minute (SLPM) zero air is metered by mass-flow controller 1 (MFC1, Type FMA-770A-V-Air, Omega Engineering) for dilution. We have used either cylinder zero air /nitrogen or room air pumped by a miniature compressor through sequential columns of indicating silica gel, soda-lime, Carulite 110TR and activated carbon.

The HCHO monitor consists of the gas sampling system, liquid delivery system, the heated reactor HR already described above, and the detection system. The gas sampling system itself consists of a diffusion scrubber (DS), mass flow controller (MFC2, FMA-768A-V-Air, Omega), air pump AP (UN86KTDCB, 12V, www.knf.com/usa.htm) and a 500 ml bottle filled with glass wool functioning as a dampener and a water trap (WT). In normal operation AP is turned on and the aspiration flow is set by MFC2 to 1 SLPM. Air aspirated through the DS sample inlet port passes through the DS and then through WT; without such a “dampener”, the flow signal is noisy. The exit air from the DS is also nearly saturated with moisture; WT also largely protects MFC2 from intrusion of condensation.

The DS is the gaseous HCHO collector and is separate from the main instrument console. It transfers gas-phase formaldehyde to the liquid phase prior to analysis. The DS construction and dimensions are schematically shown in Figure S1 in electronic supporting information (SI). A Nafion tube (Nafion 030, 0.75 mm o.d., www.permapure.com) filled with a 0.46 mm dia. nylon monofilament is centered within a 5 mm id PTFE jacket tube; this forms the heart of the DS. A glass tube outside the PTFE jacket tube helps maintain a linear configuration. The Nafion tube terminates in PTFE tubing (0.38 mm i.d., 0.84 mm o.d. 28 SW, Zeus) at both ends. The PTFE tube ends exit through the perpendicular arms of individual PVDF tees; they are sealed and glued in position using appropriate size PVC sleeve tubing and silicone adhesive. These PTFE tube ends serve as liquid inlet and outlet. The straight arm of the top PVDF tee is connected to another PVDF tee labeled as gas tee in Figure S1. The top straight arm of the gas tee serves as the ambient sample inlet in the sampling mode. The perpendicular arm (labeled as calibration source inlet line in Figure S1) is connected to the HCHO calibration source. Zero air or HCHO calibrant is provided through this arm to the DS during the calibration mode. To ensure that the same flow rate is maintained through the DS during sampling as well as sampling/zero steps, the zero/calibrant flow rate must be slightly higher than the aspiration flow rate of AP. A small amount of flow is actually vented through the straight arm during the calibration/zero mode.

Two syringe pumps (Versa 6, P/N 54002, www.Kloehn.com) are used for all liquid handling. The first syringe pump (SP1), equipped with a 2.5 ml capacity syringe (Kloehn 18780) and a 6-way distribution

valve (Kloehn P1023), is used to aspirate and dispense absorbing solution (AS) and sample carrier solution (SC). These solutions are identical, 10 mM H_2SO_4, but separate reservoirs are used. The second identically equipped syringe pump (SP2), but fitted with a 1.0 ml syringe (Kloehn 18879), is used to aspirate, mix, and dispense ammonium acetate (AA) and 2,4-pentanedione (PD) reagents. Detailed operational steps for both pumps are described in Figure S2. The minimum cycle time with which the instrument can be operated with the presently described conduit volumes is about 8 min, we used a 10 min cycle throughout this work. Any cycle period longer than 8 min can be used; with the exception of evaporative loss in the DS, the total amount of liquid reagents used per cycle is the same. Each cycle period is divided into two intervals. The first minute is the "reagent-fill period" and the rest of the cycle (9 min here) is used to dispense reagents. One of the ports of the multiport valve in SP1 is connected to a 6-port injector IV (V540, www.upchurch.com, used for liquid phase calibration and analysis) by a length of PTFE tubing (0.46 mm i.d., 0.5 m long) and IV is connected to the common port of solenoid valve SV2 (161K031, NResearch) by PTFE holding coil HC (0.46 mm i.d., 3 m long). From SP1 to SV2, a holding volume of ~600 μl is thus provided. From At t= 0, SP1 first aspirates 600 μl of fresh 10 mM H_2SO_4 directly from reservoir SC @ 5.1 ml/min. Then it switches to the port connected to IV. At t=0.27 min, SV2 is energized, connecting the common port to the DS (represented by a dotted line in Figure 1)and SP1 aspirates 600 μl solution @ 1 ml/min into HC. This results in all the absorbing solution in the DS being transferred to HC while the DS is filled with fresh absorbing solution (AS). At t=0.87 min, SV2 is turned off and connects HC to the heated reactor HR and SP1 goes idle to wait for SP2 to complete its preparation of mixed reagent filling. Control of SV2 is directly carried out by SP1 through one of the three digital outputs available from SP1 itself. While SP1 is performing its own task, SP2 alternately aspirates 20 μl of AA and 20 μl of PD repeatedly @17 ml/min for a total of 12 times so that the final volume for each reagent aspirated is 240 μl. Then SP2 dispenses the stacked liquid to a mixing chamber (MC, ~1.5 ml internal volume, with a conical bottom) at a rate of 17 ml/min. The liquid is aspirated back into the syringe at the same high speed to enhance mixing and sent back into MC one more time and again withdrawn into SP2. At t= 1 min, the mixed reagent is dispensed @ 53 μl/min through the delay chamber (DC, identical to MC, this simply increases the time needed for the reagent to reach mixing tee MT2, giving it substantial time (approximately three cycle times) for further passive mixing to occur). At t=60 s, SP1 also starts dispensing @133 μl/min, both pumps dispensing their contents simultaneously into MT2 and the merged stream flowing in to HR. The dispense rate of the individual pumps are so chosen that the rest of the cycle period goes towards exactly and completely emptying each syringe. Maintaining HR at an elevated temperature (60 ^{o}C) accelerates the formation of the fluorescent product, which proceeds to the

fluorescence detector. En route, a debubbler tee port is provided for removal of any recalcitrant gas bubbles in the detector; a low viscosity solvent like methanol can be injected through this port to remove gas bubbles.

2.3. Analysis of aqueous samples

The six-port injection valve IV permits the injection of aqueous HCHO standards to check aqueous phase analytical system performance or to perform measurement of HCHO in aqueous samples, e.g., rain, fog or cloudwater. The air pump (AP) is turned off during liquid-phase HCHO measurements. If the instrument is to be used for aqueous sample measurements for an extensive period, the DS should be disconnected altogether and AS connected directly to SV2. Formaldehyde sample solution can be loaded from the injector port to the loop (~50 l, 30 cm of 0.46 mm i.d. PTFE tubing, 26 SW, Zeus) contained in IV. After SP1 finishes aspirating AS, IV is switched to the inject position and the pumps start to dispense. The sample carrier SC transports the contents of the loop downstream and the detector response appears after the appropriate liquid transit time. Analysis of aqueous phase samples is not further separately discussed in this paper; note that injection of liquid phase samples elicit a much narrower peak due to the substantially lower dispersion involved.

2.4. Fluorescence detector

The detection system shown in Figure 3 consists of a flow-through cell constructed of black Delrin, a high-intensity blue LED (Luxeon LXHL-PB01, blue, λ_{max} 470 nm, www.lumileds.com/pdfs/DS25.pdf), a reference detector consisting of an integrated photodiode-operational amplifier combination (OPT101, www.ti.com) for monitoring the intensity of the LED, and a miniature photomultiplier tube (PMT) sensor (H5784, www.hamamatsu.com). Two large-core silica optical fibers OF (1.3 mm diameter) are used both to guide the LED light to the cell and to transmit the emitted fluorescence from the cell to the PMT. An interference filter (IF, 470 nm, 10 nm half bandwidth, www.intor.com) is placed in front of the LED to reduce the bandwidth of the LED emission spectrum. A long-pass filter (50% cutoff at 515 nm, www.edmundoptics.com) is placed in front of the PMT window to reduce scattered excitation light. The analytical reaction product, diacetyldihydrolutidine (DDL), flows to the detector, is excited by the blue light to produce green fluorescence which is carried by fiber optic OF2 to the PMT.

2.5. Data acquisition and system control

Data acquisition and control of system components are achieved through a laptop personal computer (PC, Lenovo Thinkpad X40) and a user-modifiable software based on the SoftWIRE™ platform

(www.measurementcomputing.com), a Visual BASIC based graphical user interface. The system acquires, displays and permanently stores outputs from the PMT and the reference detector through a 16-bit A/D-D/A card (DAS16/16-AO, Measurement Computing). The software also controls the two syringe pumps and SV1 via user inputs (SV2 is controlled by programmable outputs in SP1). Further, programmed outputs from the D/A card govern both the mass flow controllers; these are readily changed through the software.

2.6. Power and weight

Maximum power consumption by the instrument is 115 VAC 50/60 Hz, 60 watts. It includes three DC power supplies to power all components except the temperature controller and the heaters, which are AC powered. A 24 VDC supply (PS3, 4.5A max) is used to power both syringe pumps. A +/- 15 V DC power supply (PS2, MPJA) is used to power the mass flow controllers and the PMT. All other components, including the digital display monitor (DSP), light sources, detectors, solenoid valves and electronic circuitry, are powered by a PC power supply (PS1). The power and control flow chart for the system is shown in Figure S3.

2.7. Reagents

All chemicals are reagent grade. 2,4-Pentanedione (99%, www.sial.com) was distilled and stored refrigerated in a well-stoppered dark bottle. The working solution was prepared by diluting 3.2 ml PD with deionized water to 500 mL. Ammonium acetate solution is prepared by dissolving 240 g AA and 4.6 ml glacial acetic acid in ~300 ml water, and then diluting to 500 ml. For SC and AS 10 mM H_2SO_4 solution was prepared by adding 0.56 ml of concentrated H_2SO_4 (~98 %) to 500 ml DI water and diluting to 1-l. Required volumes for one week of continuous operation with a 10 min cycle are 1.21-l of 10 mM H_2SO_4 and 0.25-l for AA and PD each.

3. Results and discussion

3.1. Need for referencing. Light intensity stability of source LED.

It is known that although the mean times between failure of solid state light emitting sources are very long, there is a continuous decrease in output over prolonged use. The light output (and the precise λ_{max}) are also very dependent on device junction temperature (Dasgupta et al., 2003). As is also well known, the fluorescence intensity elicited is dependent directly on the excitation light intensity and its spectral distribution. Previously we have used 5 mm T-1$^3/_4$ LEDs and driven them at close to the maximum rated

currents. When operated over long periods and in environments without ambient temperature control, the reference detector output itself established that a reference detector was needed. Since that time, large junction area, very high output LEDs that are driven at very high currents and contain some integral heat sinking, have become available. We chose here to use one of these devices and to drive it at 200 mA, much less than its continuous rated maximum current of 350 mA. We expected that under such conditions there would be little degradation of light output and because such a device intrinsically operates at a high junction temperature, there will be little effect of ambient temperature. Both these expectations were realized. Four LEDs were continuously operated for 3000 h (~4 months) at a drive current of 200 mA and at the end of the test period the loss in intensity was 1.1±0.1%. We chose to operate the instruments with a LED drive current of 130 mA and there was no discernible intensity loss of calibration signal change within a two-week period, within the 0.3% relative standard deviation of the signals obtained at any given time. There was also no diurnal pattern in the reference detector output, as would have been expected if ambient temperature changes significantly affected the LED intensity. Therefore, while the reference detector output was collected and checked, no corrections were made using these data.

3.2. Homogeneity of the PD-AA mixture:

The ammonium acetate solution is very concentrated (nearly 50% w/v) and if thorough mixing is not achieved with the very dilute AA solution, artifact broad peaks are caused even when HCHO free-air is sampled. It is well known that concentration gradients from a imperfectly mixed reagent can cause Schlieren-induced artifact peaks in flow injection systems (Eom and Dasgupta, 2006). That the effect is being caused by imperfect mixing was made evident by using a premixed PD-AA solution in which case the artifact response essentially disappeared. However, a premixed solution of AA and PD is impractical because the fluorescence blank inevitably increases over time, eventually the blank gets too high for sensitive detection. The use of the mixing and the delay chambers (MC and DC) essentially provided the same performance as the premixed reagent. A small peak in the detector output is caused by the fact that the flow through the detector stops for 60 s and then resumes. This is minimized by applying a modest back pressure on the detector (by locating the waste container was located ~1 m higher than the instrument top). In any case, the stop-resume peak is much narrower compared to the sample signal and in fact occurs in a different time window, thus readily recognized either visually or by the software used for data interpretation.

3.3. Aspiration of the DS. Volume and flow rate.

When fresh absorbing solution is aspirated through the DS, the DS is filled with fresh liquid and the analyte containing absorber is transferred to HC. Since laminar, rather than plug flow is involved, there is significant axial dispersion. In addition, as HCHO actually permeates through the membrane, there is slow washout from the wall that is not encountered with an inert tube. A relatively low aspiration rate (1 ml/min) is used to minimize the laminar flow-induced band broadening. The volume of the filament-filled DS is ~80 μl. When we substituted a 0.59 mm i.d. PTFE tube of the same length as the DS with an internal volume of 105 μl, aspiration of 200 μl of fresh solution removed 96% of the original sample, resulting in ~4% carryover. In contrast, with the DS under active sampling conditions, a similar 200 μl aspiration resulted in ~23% carryover due to the slow washout from the wall. As a compromise between carryover and the total volume aspirated, we used an aspirated volume of 600 μl @ 1ml/min; this resulted in <10% carryover.

3.3. Heated reactor and permeation chamber temperature

The Hantszch reaction involves ring closure by the elimination of water and is thus accelerated at higher temperatures. The data in Figure 4 shows the effect of temperature on response. The advantage of using a higher temperature is that a shorter reaction time and a smaller volume reactor can be used, permitting better time resolution. Too high a temperature, however, leads to bubble formation in the detector; this is an issue that cannot be remotely solved and can lead to much data loss. A reaction temperature of 60 ^{o}C is relatively low but it is attractive in that the available commercial HCHO permeation devices are designed to work at this particular temperature. This then allows us to use the same heated block for the permeation tube chamber. The reaction coil volume chosen leads to a response that is 97% of the response observed at 70 °C and ~95% of the maximum response (as observed from operation at 70 °C and decreasing SP1 and SP2 dispense speeds until peak heights increased no longer.

3.4. Recovery from short term power failure.

In unattended field deployment of instruments, especially as done in measurement campaigns rather than permanent or semi-permanent installations, power failure is all too common. The use of uninterruptible power supply (UPS) units can ameliorate the problem but rarely there is more than 30 min capacity and the cost is not insignificant. Little can be done for longer term power failures. In the present instrument, controlled by a notebook PC, the PC keeps on running until its battery capacity is exhausted (typically 2-4h). The present syringe pumps have sufficient on-board memory that the control program can be downloaded into pump memory and all execution can be carried out therefrom on an infinite loop. We chose initially to

design the instrument in this fashion. But field power outages indicated that the instrument will often not restart properly, if at all. It is for this reason that except for SV2, which is linked to pump operation, none of the control commands originate with the pumps. Rather, all control commands, including instructions for both pumps to initialize themselves (power can go out when the pump is middle of dispensing) are sent out from the PC on a 10 min cycle (or whatever other cycle time is chosen). As a result, these analyzers recover well from short term power failure. Note also the reference detector output, that monitors if the LED (and hence power) is on, readily indicates the exact duration of power loss as long as the PC is still alive. Figure 5 shows several examples, from a transient one to several seconds to several minutes of power loss. In all cases, the instrument resumed operation and produced reliable data within two cycles of power return.

3.5. Performance

Four identical HCHO analyzers were constructed. All showed very good linear calibration curves over the concentration range of primary interest in ambient measurements (0 – 50 ppbv), with all r^2 values $\geq$ 0.9960. Figure 6 shows typical output from a calibration series for one instrument. Note that the first peak of multiple repeated measurements is always discernibly lower than the rest in an ascending calibration series because of carryover. The limit of detection (LOD, S/N =3) varied by a factor of 2 from the best (0.06 ppbv) to the worst (0.12 ppbv) essentially because of differences in the fluorescence detector S/N. The exact placement of the fiber optic etc. within FC do affect the performance. No efforts were made to improve this further even for the poorest performer, as this LOD was deemed generally adequate to measure ambient levels of HCHO.

When calibrated from a common source and deployed within the same laboratory sampling indoor air, the worst disagreement over several hours was 4.4% between instruments. On the average, the standard deviation of the data produced by the three instruments was 3.2% at a mean indoor HCHO level of 7 ppbv. Two instruments were then used to monitor outdoor HCHO levels while a third one monitored indoor levels to ascertain if indoor levels are affected by the infiltration of outdoor air and how well the two independent monitors track each other. Figure 7 shows that the two analyzers collocated in our laboratory and sampling ambient outdoor air in Lubbock, TX were in very good agreement (the slope of the best fit line when the two sets of data are plotted against each other is 1.01. The concurrent data for the third analyzer does not suggest that infiltration of outdoor air have much to do with indoor HCHO levels.

3.6. Field deployment and field data.

Three instruments were located in three urban areas in Texas in the summer of 2006 for extended periods. This included Meacham field near Ft. Worth, TX (Lat/Long. : 32.8197778°/-97.3624444°, http://en.wikipedia.org/wiki/Fort_Worth_Meacham_International_Airport) from September 1 to October 30, 2006, United States Environmental Protection Agency site number 48-201-1015, Baytown, TX (Lynchburg Ferry site, CAMS 1015, Lat/Long. : 29.764444°,-95.077778°, http://www.tceq.state.tx.us/cgi-bin/compliance/monops/site_photo?1015) and United States Environmental Protection Agency site number 48-201-0803, Houston, TX (HRM-3 site, CAMS 603, Lat/Long.: 29.765278°/-95.181111°, http://www.tceq.state.tx.us/cgi-bin/compliance/monops/site_photo?603), both from August 22 to October 14, 2006. The two latter sites have criteria pollutant data, as well as other data continuously collected that are accessible through the web (http://www.tceq.state.tx.us/cgi-bin/compliance/monops/daily_summary). Location of the sites in Central and Eastern Texas are shown in Figure S4 in SI. Intermittent or sustained power failure/brownout issues plagued all the sites to different degrees, leading us to provide the software fix through the middle of the deployment protocol such that the effect of intermittent power failure were minimized. Two of the three units were also protected with UPS units. The instruments provided extensive data over the measurement campaign; these are presented in SI. The maximum and average concentrations during the study period were, respectively 19 and 3.6 ppb (Meacham), 52 and 7.1 ppb (Lynchburg Ferry) and 31.5 and 4.4 ppb (HRM-3). The overall pattern of the data at the latter two sites is shown in Figure S5. Details of one week's worth of data from the latter two sites surrounding the occasion of the highest HCHO excursion on September 27 are shown in Figure S6 in color, with the inset showing the location of the two sites, HRM3 being 12 km due west of Lynchburg Ferry. For clarity, only three days worth of data are similarly presented here in Figure 8. While a detailed rationalization of the data are beyond the scope of the present paper, we deem the following to be worthy of mention. First, the ozone excursions at the two sites are of the same general magnitude while the HCHO concentrations vary markedly. Second, the ozone maxima always occur significantly after the formaldehyde maxima suggesting the ozone is being produced over a much larger region than the temporally (and presumably spatially) narrow windows of HCHO excursions – if bulk of the ozone is not being produced and transported into the measurement sites it will be difficult to account for the HCHO as originating from ozonolysis of olefins. Third, from the fact that similar HCHO patterns are often observed at the HRM-3 site as the Lynchburg Ferry site, only somewhat later and sometime diminished (see e.g., 10 am –noon and 6-9 pm on Sep 26) it may be tempting to conclude that the same air mass is transported from one site to the other. However, this is not the case. In the first instance, the prevailing wind direction on both sites was from NNE to NE and in the latter case, wind was from due S, bringing the same ship channel emissions at

different times to the two sites. Preceding and during the highest HCHO excursion on the morning of the 27th, the wind was also generally from the South. Although other high levels of HCHO occurrence has been reported for the Houston area (Dasgupta et al., 2005; Chen et al., 2004), to our knowledge, the 52 ppbv concentration measured at Lynchburg Ferry sets a new record. Finally, of considerable interest is the period of midnight - ~8 am on Sep 27 when ozone levels are so low at both sites that it would appear that ozone was being titrated. Indeed, this was the case – the data in supplementary information shows that there were large emissions of NO, reaching e.g., 109 ppbv of NO at 4 am on the Lynchburg Ferry site. There were similar NO peaks at HRM-3. During this period, there are large periodic excursions of HCHO at the Lynchburg Ferry site but not at the HRM-3 site. At the present time, this is not fully understood. During the preceding several hours, the wind was from the south. From midnight to 8 am, the wind changed from WSW to NNW, which would allow some of the previously advected air mass to return. However, the wind pattern was largely the same as both sites (as also seen from the NOAA HYSPLIT models) and cannot explain the significant difference between the two sites. It is possible that primary HCHO emissions (Friedfield et al., 2002) play a role but it seems to us that there are likely other reasons that we cannot presently explain.

In summary, we provide here the details of performance and construction of a robust self-calibrating automated atmospheric HCHO analyzer. A complete instrument manual and software codes are provided in SI. Extensive field data were obtained and are available in SI for future researchers.

ACKNOWLEDGMENT

This research was supported by a grant from the Texas Commission on Environmental Quality. However, no endorsement by the agency should be inferred.

Appendix A. Supplementary data

Supplementary data associated with this article can be found in the online version at xx.xxxx/j.atmosenv.200x.yy.0zz.

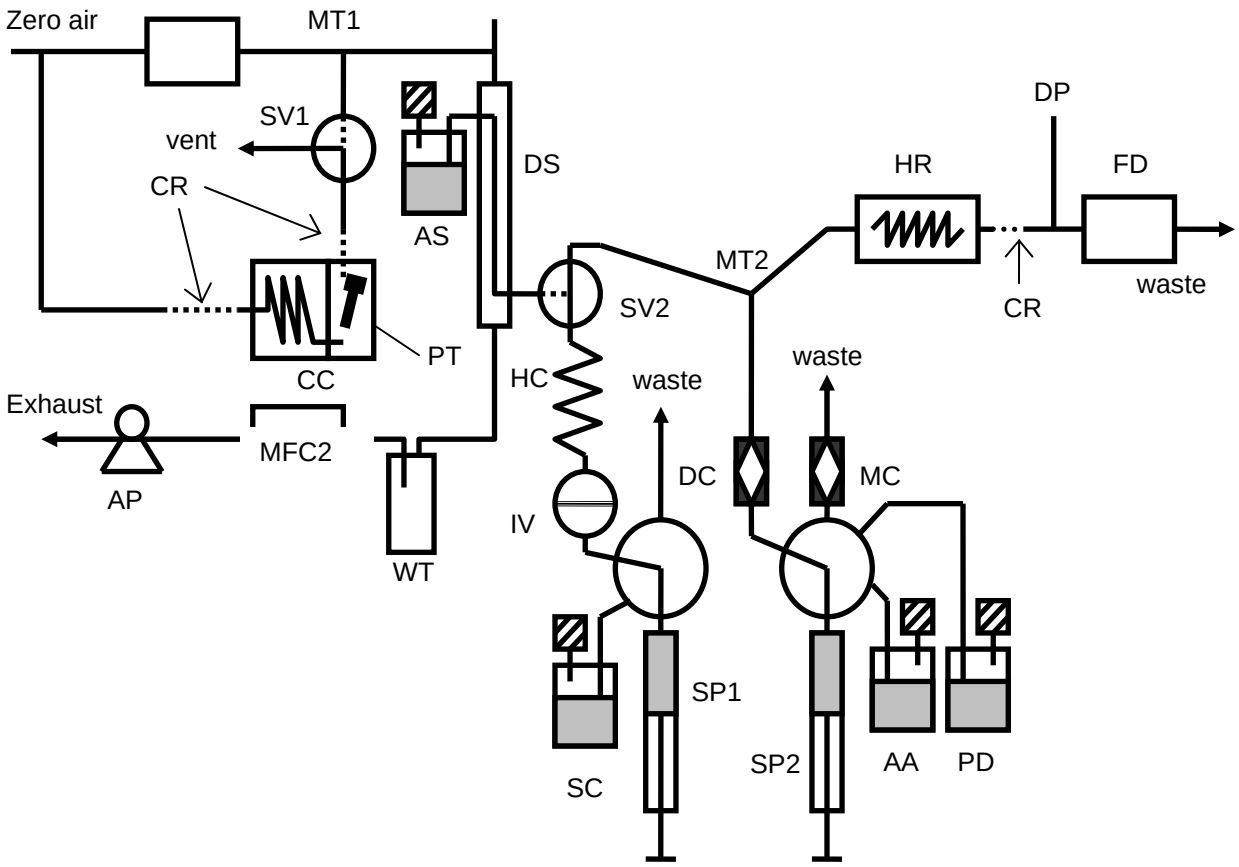

Figure 1. Overall system schematic for gaseous HCHO measurement. MFC1: mass-flow controller for dilution of the HCHO calibration source; MFC2: mass-flow controller for sampling air, usually fixed at 1 SLPM; CC: calibrant chamber containing HCHO permeation tube; DS: diffusion scrubber; HR: heated reactor, maintained at 60 ^{o}C; FD: fluorescence detector; HC: holding coil; MC: mixing chamber; DC: delay chamber; SP1 and SP2: syringe pumps for liquid handling; IV: injection valve (six-way) for liquid phase HCHO measurement; AS: absorbing solution (10 mM H_2SO_4) for gaseous HCHO sampling; SC: sample carrier solution (10 mM H_2SO_4) for establishing baseline; AA: ammonium acetate solution; PD: pentanedione solution; SV1: solenoid valve for sampling /calibration switching; SV2: solenoid valve for aspirating and dispensing the DS absorbing solution (AS); CR: capillary (100 μm id) restrictor for gas and liquid flows (see text for details); AP: air pump for sampling; WT: water trap for protecting MFC2; MT: mixing tees for gas (MT1) and liquid (MT2); DP; debubble port.

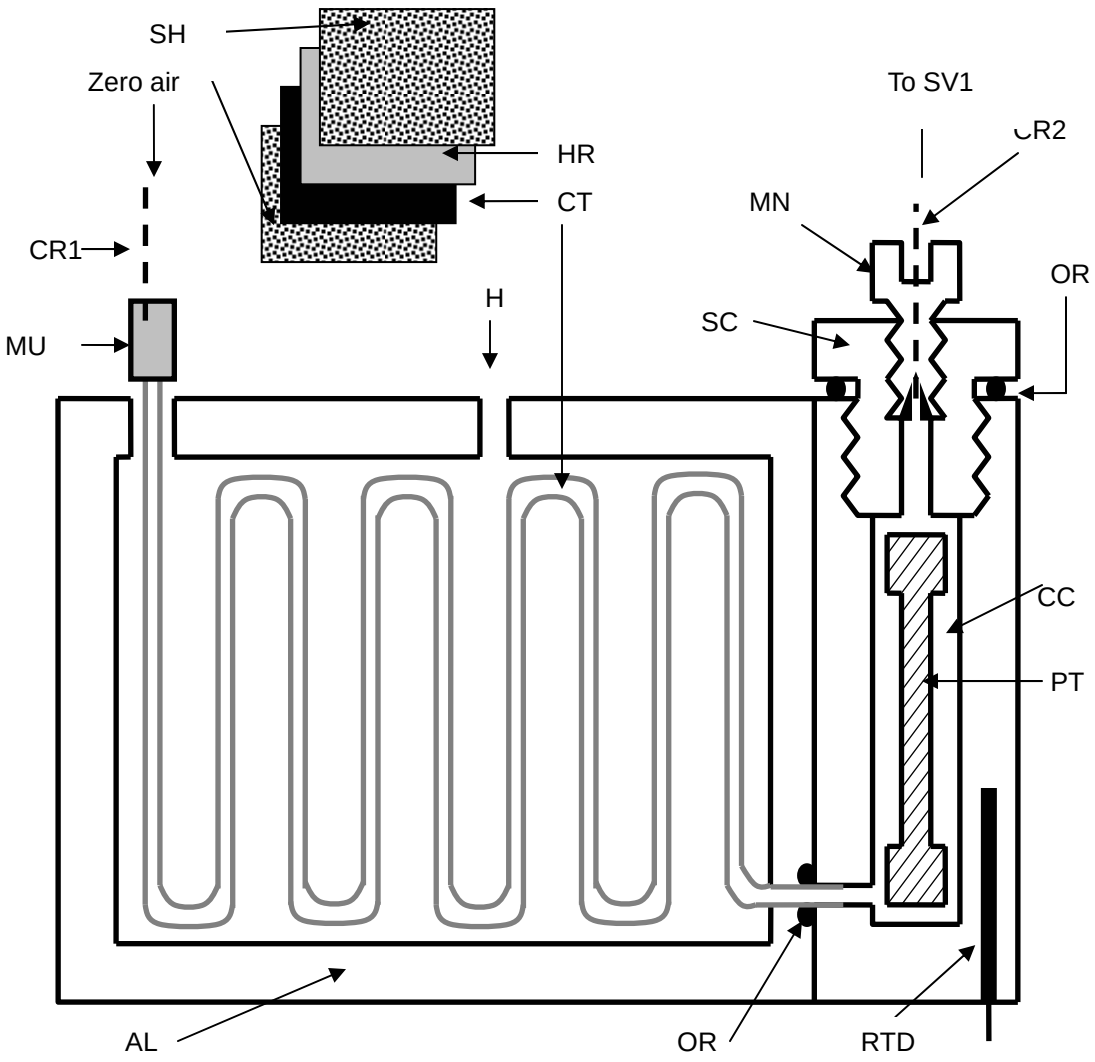

Figure 2. Schematic of heated reactor and permeation chamber. Left compartment holds the heater, reaction coil, and copper tubing; SH: flexible siliconized heater on top and bottom; HR: heated reaction coil layer; CT: shaped copper tubing (~60 cm, 3/8”) for preheating the purge zero air; CR: capillary restrictor; MU: metal union; H: exit aperture for guiding HR inlet and outlet terminal tubing; SC: screw cap: OR: O-ring; MN: ¼ 28 threaded male nut; CC: calibrant chamber containing a HCHO permeation tube PT; RTD: platinum resistance-temperature device; AL: main Aluminum body.

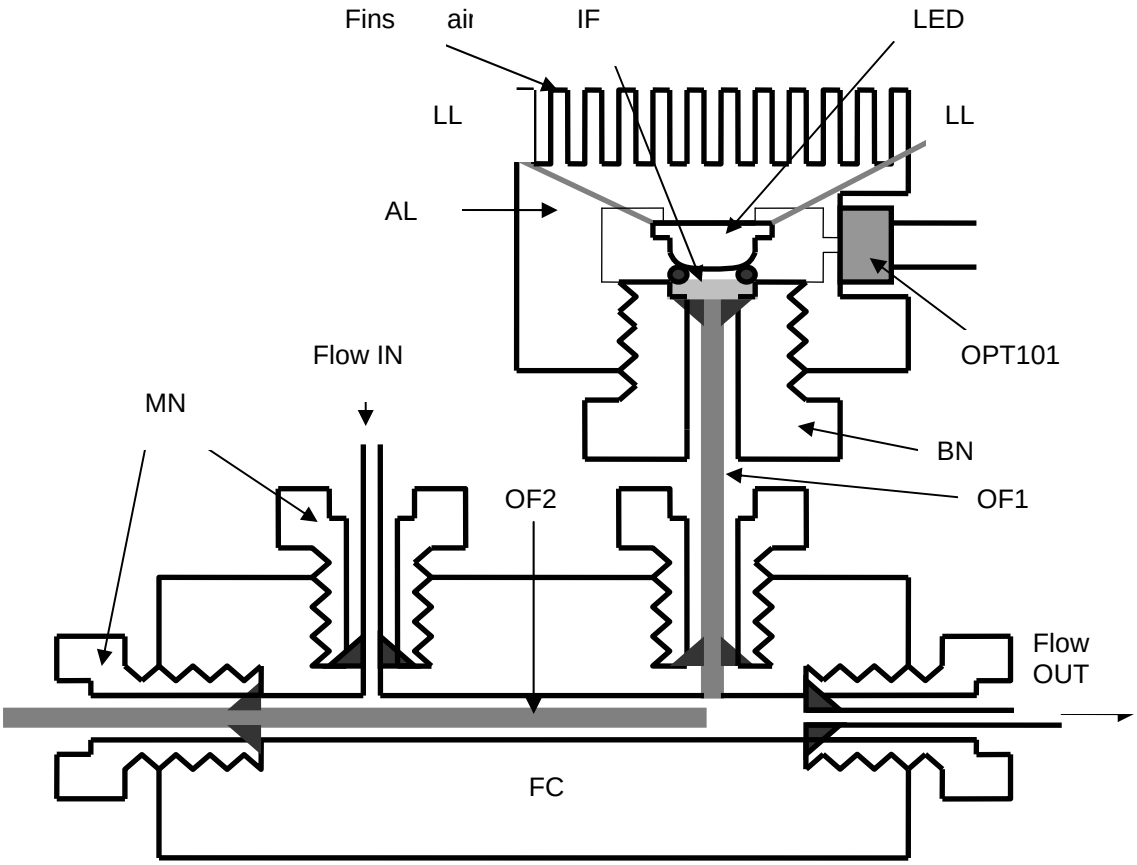

Figure 3. Fluorescence detector schematic. LED:light emitting diode; LL: LED leads; AL: aluminum holder for LED acting as a finned heat sink; OPT101: photodiode with integrated operational amplifier; OF; optical fibers, OF1 delivers source light and OF2 receives fluorescence produced and guides it to the PMT window; BN: black plastic nut holding OF; FC: flow-through cell; MN: ¼ 28-threaded male nut; IF: 470 nm interference filter.

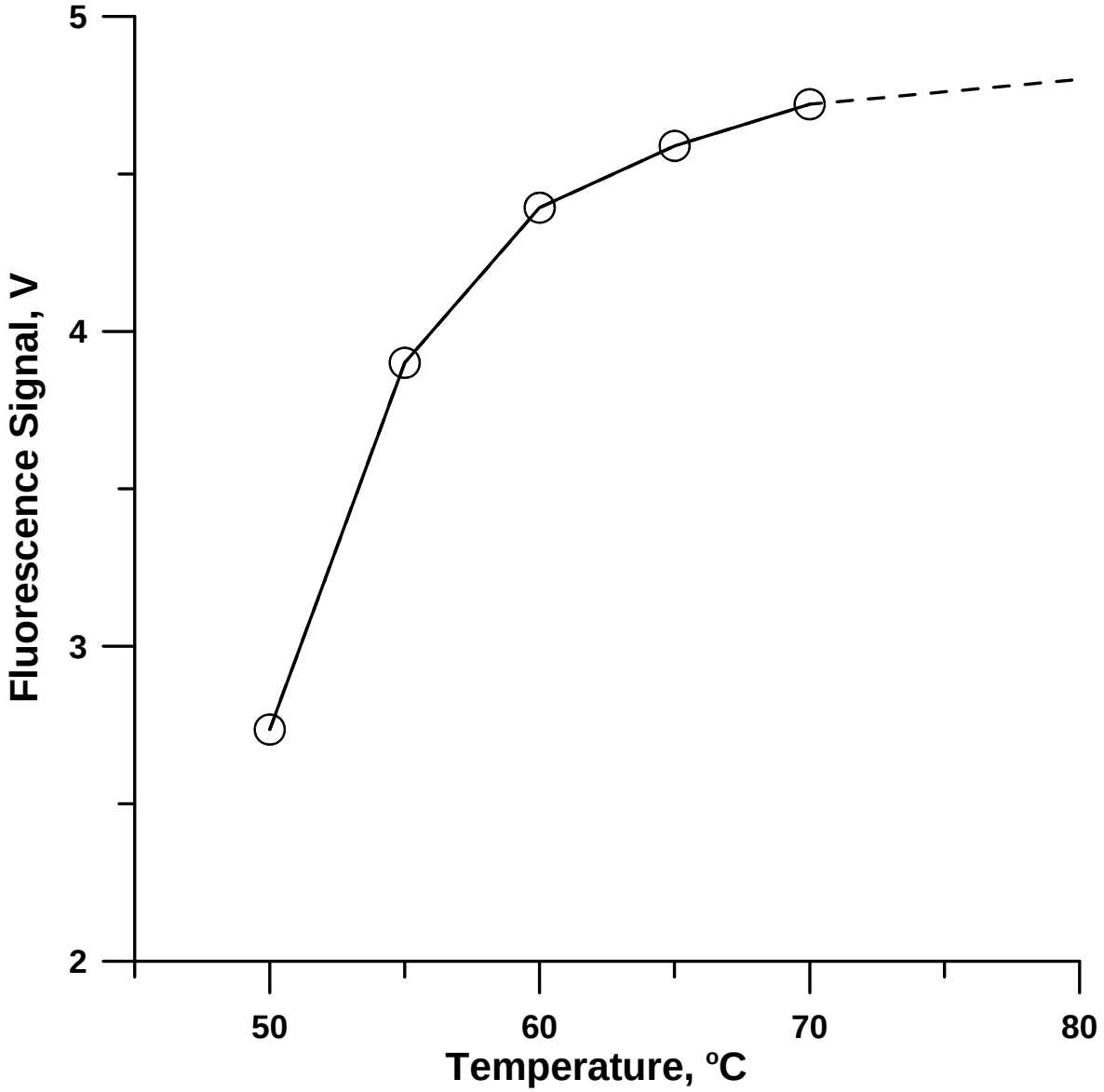

Figure 4. Fluorescence response versus temperature of the heated reactor. The dotted line extends the response to the maximum response observed by slowing the flow down.

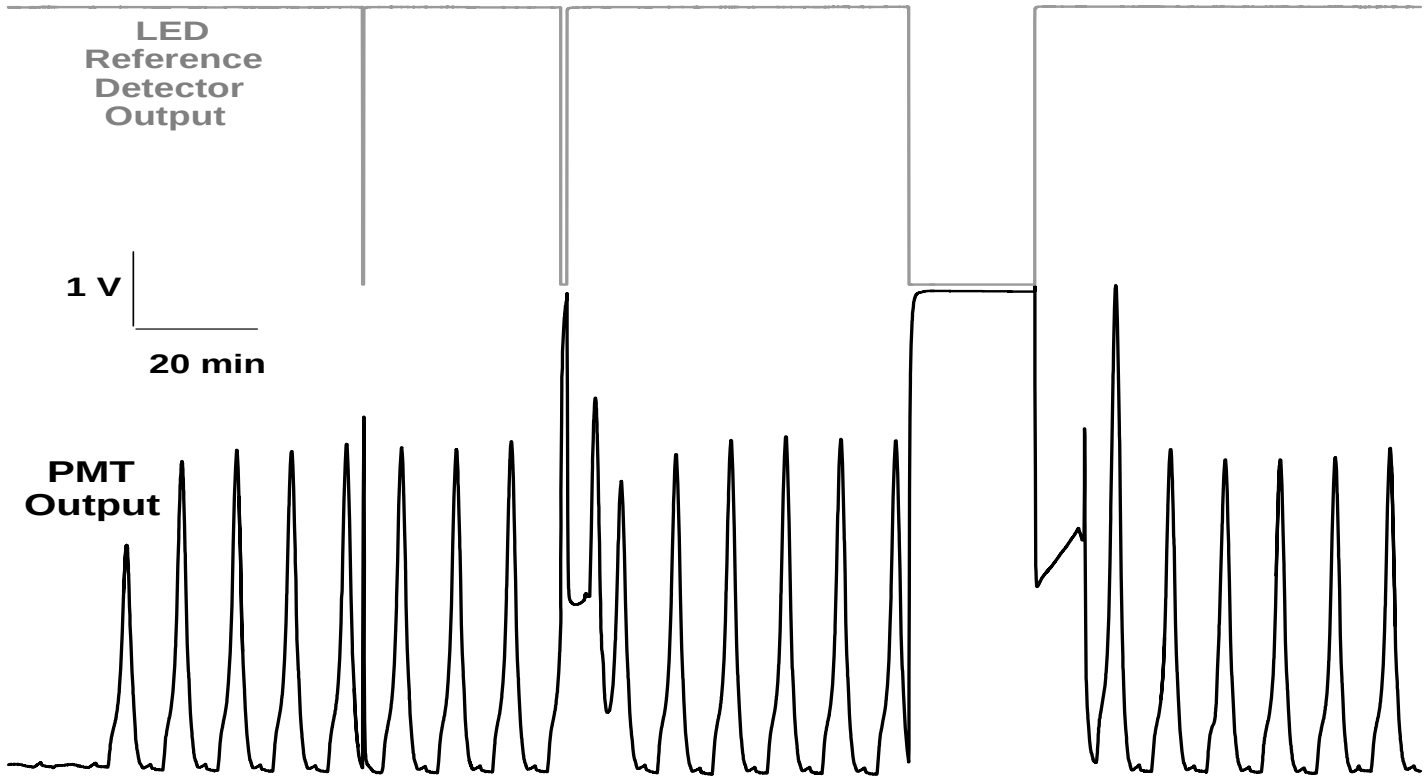

Figure 5. Recovery from short-term power failure. The instrument is sampling ~20 ppbv HCHO. Usable data production is resumed 1-2 cycles after power restoration.

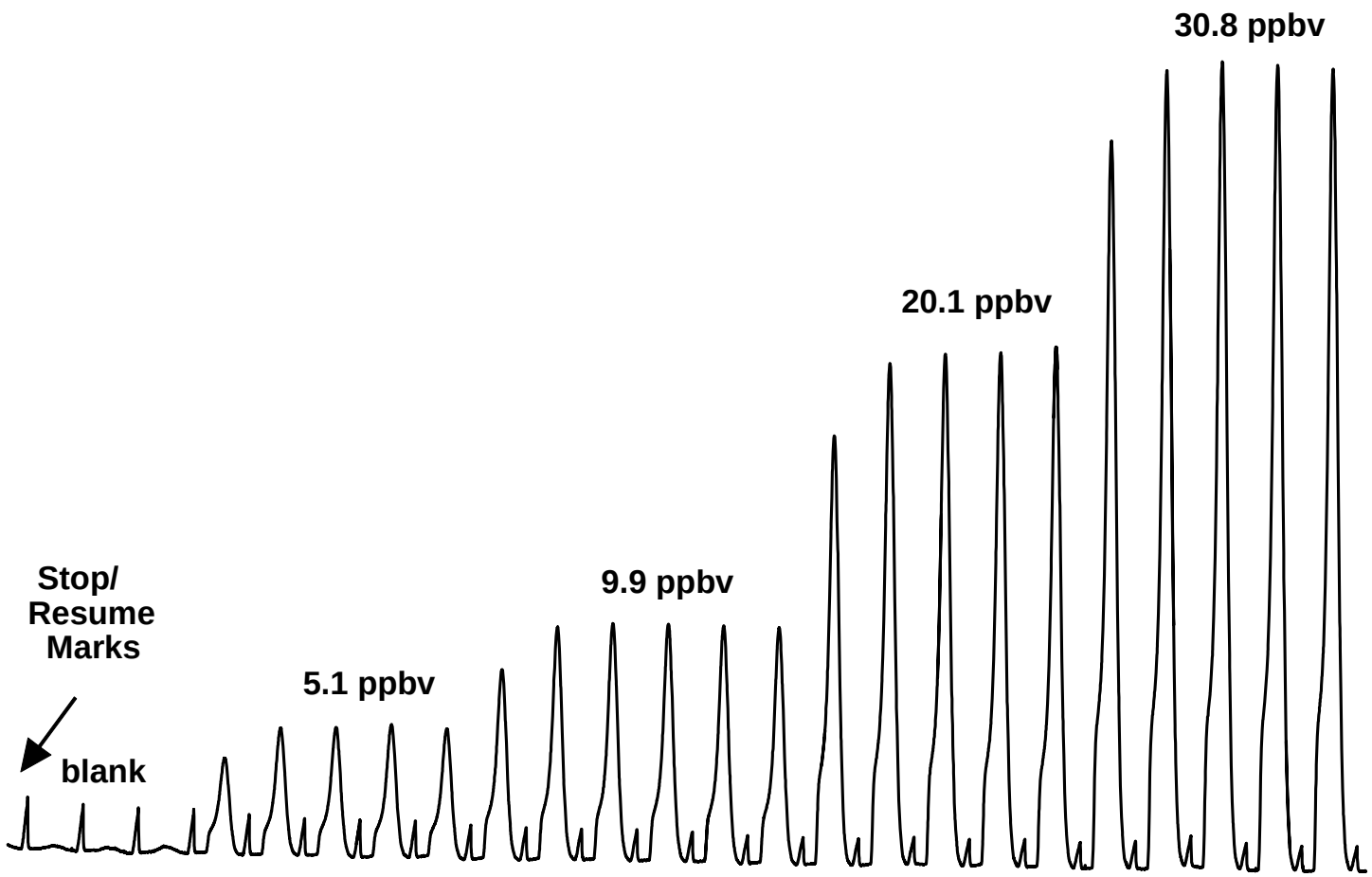

Figure 6. Programmed automated calibration series output for Analyzer 03.

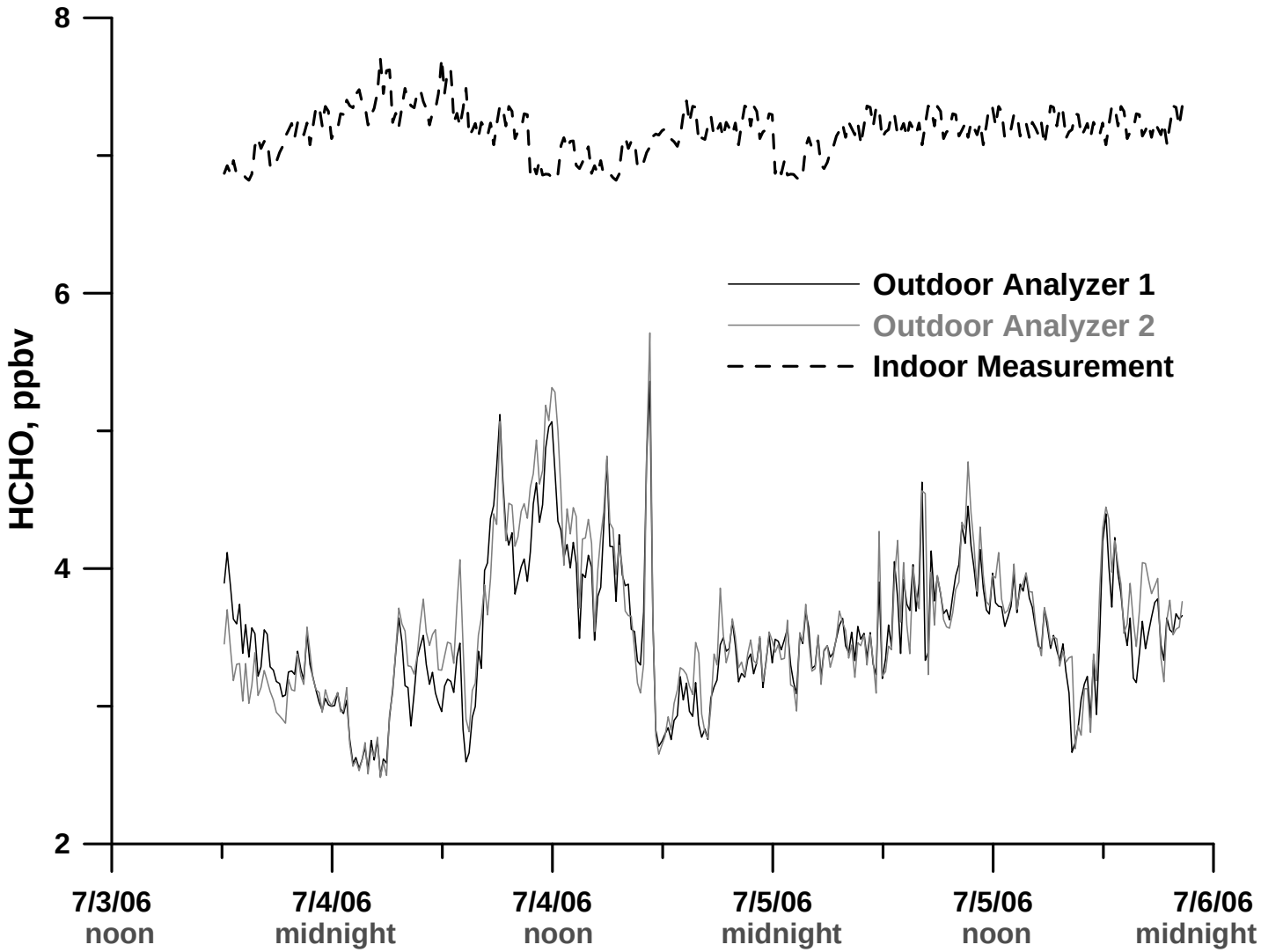

Figure 7. Outdoor sampling results by two HCHO analyzers with simultaneous indoor sampling by a third analyzer

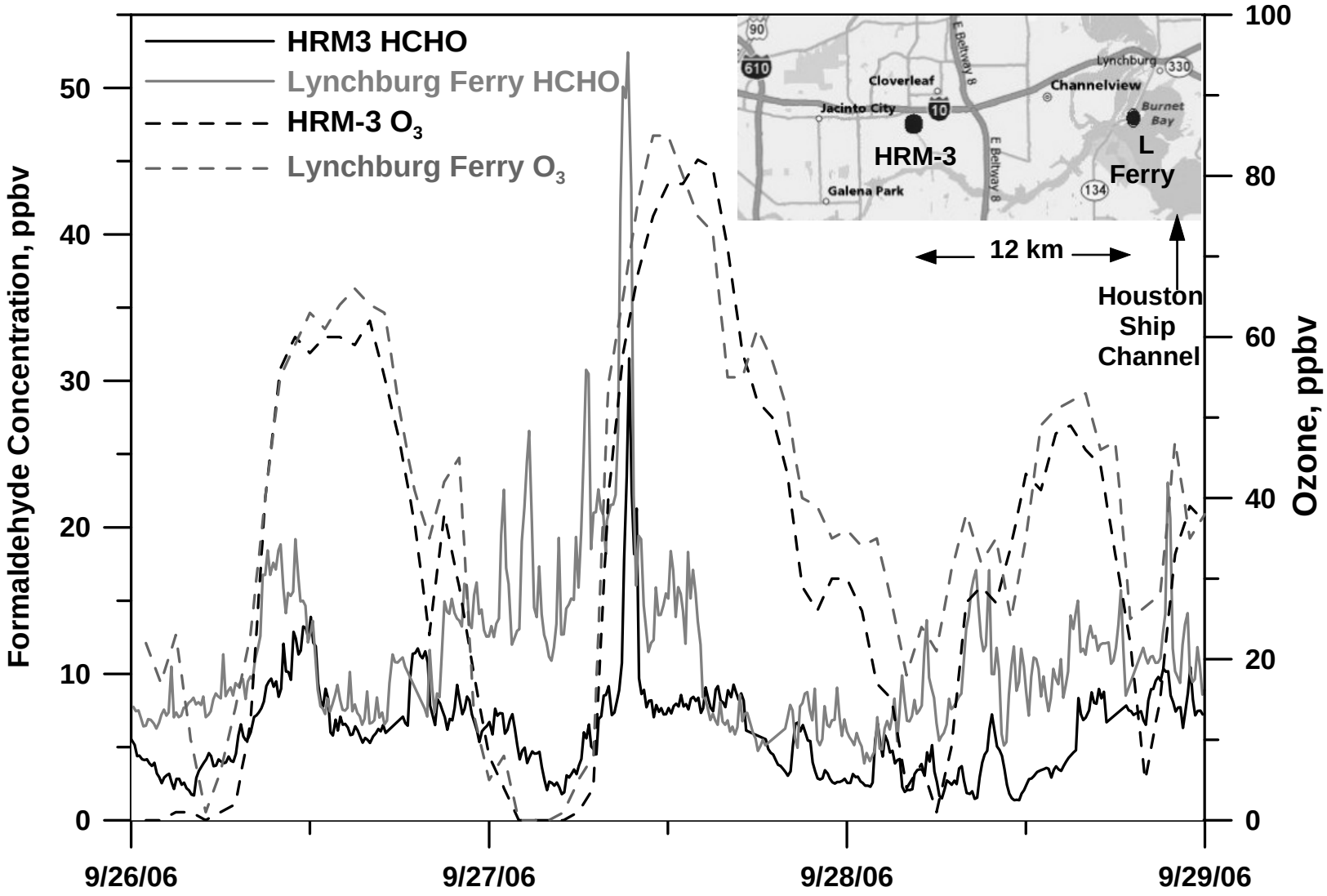

Figure 8. Three days of 10 min HCHO and hourly ozone concentrations surrounding the maximum HCHO excursions observed at HRM-3 and Lynchburg Ferry sites.

References

Amornthammarong, N., Jakmunee, J., Li, J., Dasgupta, P.K. 2006. Hybrid fluorometric flow analyzer for ammonia. Analytical Chemistry 78, 1890-1896.

Chen, J. H, So, S., Lee, H.S., Fraser, M.P., Curl, R.F., Harman, T., Tittel, F.K. 2004. Atmospheric formaldehyde monitoring in the greater Houston area in 2002. Applied Spectroscopy 58, 243-247.

Dasgupta, P.K. 1987. Application of continuous liquid phase fluorescence analysis for the selective detection of gases. Proceedings of the International Society of Optical Engineering. 743, 97-102.

Dasgupta, P.K., Dong, S., Hwang, H., Yang, H., Zhang, G. 1988. Continuous liquid-phase fluorometry coupled to a diffusion scrubber for the real-time determination of atmospheric formaldehyde, hydrogen peroxide and sulfur dioxide. Atmospheric Environment 22, 949-963.

Dasgupta, P.K., Dong, S., Hwang, H. 1990. Diffusion scrubber-based field measurements of atmospheric formaldehyde and hydrogen peroxide. Aerosol Science and Technology 12. 98-104.

Dasgupta, P.K., Eom, I.-Y., Morris, K.J., Li, J. 2003. Light emitting diode based detectors. Absorbance, fluorescence and spectroelectrochemical measurements in a planar flow-through cell. Analytica Chimica Acta 500, 337-364.

Dasgupta, P.K., Li J.; Zhang, G., Luke, W.T., MacClenny, W.A., Stutz, J., Fried, A. 2005. Summertime ambient formaldehyde in five U.S. metropolitan areas: Nashville, Atlanta, Houston, Philadelphia, and Tampa. Environmental Science and Technology 39, 4767-4783.

Dong, S., Dasgupta, P.K. 1986a. Solubility of gaseous formaldehyde in liquid water and generation of trace standard gaseous formaldehyde. Environmental Science and Technology 20, 637-640.

Dong, S., Dasgupta, P.K. 1986b.On the formaldehyde-bisulfite-hydroxymethanesulfonate equilibrium. Atmospheric Environment 20, 1635-1637.

Dong, S., Dasgupta, P.K. 1987. Fast fluorometric flow injection analysis of formaldehyde in atmospheric water. Environmental Science and Technology 21, 581-588.

Eom, I.-Y., Dasgupta, P.K. 2006. Frequency-selective absorbance detection: Refractive index and turbidity compensation with dual wavelength measurement, Talanta 69, 906-913.

Fan, Q., Dasgupta, P.K. 1994. Continuous automated determination of atmospheric formaldehyde at the parts per trillion level. Analytical Chemistry 66, 551-556.

Friedfeld, S., Fraser, M., Ensor, K., Tribble, S., Rehle, D., Leleux, D., Tittel F. 2002. Statistical analysis of primary and secondary atmospheric formaldehyde. Atmospheric Environment 36, 4767-4775.

Gilpin, T., Apel, E., Fried, A., Wert, B., Calvert, J.. Genfa, Z., Dasgupta, P.K., Harder, J.W.. Heikes, B.G., Hopkins, B., Westberg, H., Kleindienst, T., Lee, Y.-N., Zhou, X., Lonneman, W., Sewell, S. 1997. Intercomparison of six ambient [CH_2O] measurement techniques. Journal of Geophysical Research – Atmospheres 102, 21161-21188.

Grutter, M., Flores, E., Andraca-Ayala, G., Baez, A. 2005. Formaldehyde levels in downtown Mexico City during 2003. Atmospheric Environment 39, 1027-1034.

Kleindienst, T.E., Shepson, P.B., Nero, C.M., Arnts, R.R., Tejada, S.B., MacKay, G.I., Mayne, L.K., Schiff, H.I., Lind, J.A., Kok, G.L., Lazrus, A.L., Dasgupta, P.K., Dong, S. 1988. An Intercomparison of Formaldehyde Measurement Techniques at Ambient Concentration. Atmospheric Environment 22, 1931-1939.

Koziel, J.A., Noah, J., Pawliszyn, J. 2001. Field sampling and determination of formaldehyde in indoor air with solid-phase microextraction and on-fiber derivatization. Environmental Science and Technology 35, 1481-1486.

Lawson, D.R., Biermann, H. W., Tuazon, E.C., Winer, A.M., Mackay, G.I., Schiff, H.I., Kok, G.L., Dasgupta, P.K., Fung, K. 1990. Formaldehyde Measurement Methods Evaluation and ambient concentrations during the carbonaceous species methods comparison study. Aerosol Science and Technology 12, 64-76.

Lee, C., Kim, Y., Hong, S., Lee, H., Jung, J., Choi, Y., Park, J., Kim, K., Lee, J., Chun, K.; Kim, H. 2005. Measurement of atmospheric formaldehyde and monoaromatic hydrocarbons using differential optical absorption spectroscopy during winter and summer intensive periods in Seoul, Korea. Water Air and Soil Pollution 166, 181-195.

Li, J., Dasgupta, P.K., Zhang, G., Hutterli, M.A. 2001. Measurement of atmospheric formaldehyde with a diffusion scrubber and light-emitting diode-liquid-core waveguide based fluorometry. Field Analytical Chemistry and Technology 5, 2-12.

Li, J., Dasgupta, P.K., Luke, W. 2005. Measurement of gaseous and aqueous trace formaldehyde. Revisiting the pentandione reaction and field applications. Analytica Chimica Acta 531, 51-68.

Liu, S., Dasgupta, P.K. 1995. Electroosmotically pumped capillary format sequential injection analysis with a membrane sampling interface for gaseous analytes. Analytica Chimica Acta 308, 281-285.

Ohira, S.-I.; Li, J.; Lonneman, W.A., Dasgupta, P.K., Toda, K. 2007. Can breath isoprene be measured by ozone chemiluminescence? Analytical Chemistry 79, 2641-2649.

Pereira, E.A., Dasgupta, P.K. 1997. Measurement of atmospheric formaldehyde using a drop collector and in-situ colorimetry. International Journal of Environmental Analytical Chemistry 66, 201-213.

Pretto, A., Milani, M.R., Cardoso, A.A. 2000. Colorimetric determination of formaldehyde in air using a hanging drop of chromotropic acid, Journal of Environmental Monitoring 2, 566-570.

Roller, C., Fried, A., Walega, J., Weibring, P., Tittel, F. 2006. Advances in hardware, system diagnostics software, and acquisition procedures for high performance airborne tunable diode laser measurements of formaldehyde. Applied Physics B 82, 247-264.

Samanta, G., Zhang, S., Dasgupta, P.K. 2003. An automated sequential injection analysis system for the determination of trace endotoxin levels in water. PDA Journal of Pharmaceutical Science and Technology 57, 12-24.

U.S. Environment Protection Agency, 1999. Compendium of methods for the determination of toxic organic compounds in ambient air, Method TO-11A, EPA-625/R-96/010b.

US Environmental Protection Agency, 2006. Chemicals evaluated for carcinogenic potential by the Office of Pesticide Programs. http://envirocancer.cornell.edu/turf/chemseval.pdf

US Environmental Protection Agency, 2007. An Introduction to Indoor Air Quality. Formaldehyde. http://www.epa.gov/iaq/formalde.html

Waiz, S., Cedillo, B.M., Jambunathan, S., Hohnholt, S.G., Dasgupta, P.K. Wolcott, D.K. 2001. Dispersion in open tubular reactors of various geometries. Analytica Chimica Acta 428, 163-171.

Wang, Q., O'Reilly, J., Pawliszyn, J. 2005. Determination of low-molecular mass aldehydes by automated headspace solid-phase microextraction with in-fiber derivatization, Journal of Chromatography 1071, 147-154.

Wert, B.P., Trainer, M., Fried, A., Ryerson, T.B., Henry, B. Potter, B., Angevine, W.M., Atlas, E., Donnelly, S.G., Fehsenfeld, F.C., Frost, G.J., Goldan, P.D., Hansel, A., Holloway J.S., Hubler, G., Kuster, W.C., Nicks, D.K., Neuman J.A., Parrish, D.D. Schauffler, S., Stutz, J., Sueper, D.T., Wiedinmyer C., Wisthaler, A. 2003a. Signatures of terminal alkene oxidation in airborne formaldehyde measurements during TexAQS 2000. Journal of Geophysical Research - Atmosphere 108(D3), Art. no. 4104.

Wert, B.P., Fried, A., Rauenbuehler, S.; Walega, J., Henry, B. 2003b. Design and performance of a tunable diode laser absorption spectrometer for airborne formaldehyde measurements. Journal of Geophysical Research – Atmospheres 108(D12), Art. No. 4350.

Zhang, G., Dasgupta, P.K. 1991. Design of a straight inlet diffusion scrubber. Comparison of particle transmission with other collection devices and characterization for the measurement of hydrogen peroxide and formaldehyde. Atmospheric Environment 25, 2717-2729.